EFFECT OF ROTATION ON INTERNAL COOLING OF GAS TURBINE BLADES

PREETAM DEBASISH SAHA ROY

EFFECT OF ROTATION ON INTERNAL COOLING OF GAS TURBINE BLADES

Thesis submitted to
Indian Institute of Technology Kharagpur
For the award of the degree

of

Master of Technology
in
Thermal Science and Engineering

by

Preetam Debasish Saha Roy

Roll No. 12ME62R15

Under the guidance of

Prof. Abhijit Guha

DEPARTMENT OF MECHANICAL ENGINEERING
INDIAN INSTITUTE OF TECHNOLOGY KHARAGPUR
APRIL 2014

Department of Mechanical Engineering

Indian Institute of Technology Kharagpur

APPROVAL OF THE VIVA-VOCE BOARD

Date:

Certified that the thesis entitled **"Effect of Rotation on Internal Cooling of Gas Turbine Blades"** submitted by **Preetam Debasish Saha Roy** (12ME62R15) to the Indian Institute of Technology, Kharagpur, for the award of the degree Master of Technology in Thermal Science and Engineering has been accepted by the external examiner and that the student has successfully defended the thesis in the viva-voce examination held today.

(External Examiner)

PROF. ABHIJIT GUHA

Department of Mechanical Engineering

Indian Institute of Technology, Kharagpur

Department of Mechanical Engineering

Indian Institute of Technology, Kharagpur

CERTIFICATE

This is to certify that the thesis entitled **"Effect of Rotation on Internal Cooling of Gas Turbine Blades"**, submitted by **Preetam Debasish Saha Roy** (12ME62R15) to Indian Institute of Technology, Kharagpur, is a record of bona fide research work under my supervision and I consider it worthy of consideration for the award of the degree of Master of Technology in Thermal Science and Engineering.

Date: 30-04-2014

Place: Kharagpur

PROF. ABHIJIT GUHA

Department of Mechanical Engineering

Indian Institute of Technology, Kharagpur

DECLARATION

I certify that

a. The work contained in the thesis is original and has been done by myself under the general supervision of my supervisor(s).
b. The work has not been submitted to any other Institute for any degree or diploma.
c. I have followed the guidelines provided by the Institute in writing the thesis.
d. I have conformed to the norms and guidelines given in the Ethical Code of Conduct of the Institute.
e. Whenever I have used materials (data, theoretical analysis, and text) from other sources, I have given due credit to them by citing them in the text of the thesis and giving their details in the references.
f. Whenever I have quoted written materials from other sources, I have put them under quotation marks and given due credit to the sources by citing them and giving required details in the references.

Signature of the Student

ACKNOWLEDGEMENT

I would like to express my sincere gratitude to my advisor **Prof. Abhijit Guha** for his guidance throughout this research work. He has always been a constant source of inspiration in all my endeavours at IIT Kharagpur. His timely inputs, motivation and significant suggestions have helped me a lot in this work. He is a symbol of dedication and excellence.

I am grateful to my parents who have always been my sources of support and inspiration.

I would like to thank all my seniors, friends and well wishers who helped me by giving important suggestions at hard times.

Preetam Debasish Saha Roy

CONTENTS

NOMENCLATURE

v	velocity (m/s)
ω	angular velocity (rad/s)
ρ	density (kg/m^3)
p	pressure (N/m^2)
μ	dynamic viscosity (kg/m.s)
T	temperature (K)
Re	Reynolds Number
D_h	hydraulic diameter (m)
Ro	Rotation N umber
KE	kinetic energy
PE	potential energy
L	length of the coolant channel
g	gravitational acceleration (m/s^2)
c_p	specific heat capacity at constant pressure (J/kg-K)
e	mid span radius (m)
D	diameter of the coolant channel (m)
R_C	radius of the coolant channel (m)
h	heat transfer coefficient (W/m^2 -K)
S	wetted perimeter (m)
m_c	coolant mass flow rate (kg/s)
U	overall heat transfer coefficient (W/m^2 -K)
y^+	dimensionless wall distance
u^*	friction velocity (m/s)
τ_w	shear stress (N/m^2)

Nu	Nusselt Number
Pr	Prandtl Number
η	cooling efficiency
ε	cooling effectiveness
m^*	non-dimensional coolant mass flow rate

Subscripts

Dh	hydraulic diameter (m)
rel	with respect to rotating reference frame of reference
0	total properties
c	coolant
i	inlet
o	outlet
g	gas
$root$	the root of the blade
tip	the blade tip
nr	non-rotating case
r	rotating case

LIST OF FIGURES

LIST OF TABLES

ABSTRACT

Quantitative analysis and a detailed physical understanding of the turbine blade cooling are important for the determination of performance and life of a gas turbine power plant. In this work a new analytical theory has been formulated to include the effect of blade rotation on the heat transfer to the cooling fluid. It is shown that depending on the flow parameters the predicted value of the change of the coolant relative total temperature can be significant when rotation is included in the analysis. A detailed computational fluid dynamic (CFD) simulation of conjugate heat transfer with blade rotation has also been performed. The computations show intricate interaction of centrifugal force, Coriolis force and heat transfer characteristics giving rise to non-uniform secondary flow pattern within the coolant flow passages. The surface-averaged heat transfer characteristics determined from the present CFD computation match well with the new analytical theory developed here.

CHAPTER 1
INTRODUCTION

1.1. INTRODUCTION

Improvement in the performance of aero-engine gas turbines and ground based gas turbines may be achieved by increasing the thrust per unit air flow, increasing the thermal efficiency and improving fuel consumption characteristics. As the thermal efficiency increases with increasing turbine inlet temperature (up to a certain limit [1]), there has been a continuous strive towards higher turbine inlet temperatures throughout the history of gas turbines. The turbine inlet temperatures in operation have increased from about 740K in the early days to 1500-1700K in modern gas turbine engines. The turbine inlet temperature that an engine achieves is such a significant factor in determining its performance that it is a closely guarded industrial secret.

A high turbine inlet temperature leads to high thermal stresses in the blade and may lead to material failure. Turbine inlet temperatures of modern gas turbines are far higher than the melting point of the blade material (nickel and cobalt based alloys). Additionally, due to rotation the turbine blades are also subjected to mechanical stresses. So, sophisticated blade cooling techniques are employed to achieve these high turbine inlet temperatures without reducing the blade life. The turbine blades are cooled by bleed air from high pressure compressors bypassing the combustion chamber. An increased turbine inlet temperature requires a higher degree of cooling which can be achieved by increasing the mass flow rate of air bled from the high pressure compressors. In modern gas turbine engines the proportion of bled air can be as high as 25% of the total air flow rate. But this bleed air imposes a penalty on the cycle efficiency as this air does not take part in combustion. Too small coolant air flow rate causes higher blade temperature and lowers component life, while too large a coolant flow rate reduces the thermal efficiency, thus affecting engine performance. Also, turbine blade cooling also needs to be considered in final stages of design for systematic

thermodynamic optimization of the engine performance [2]. Therefore, optimization of the cooling air flow rate is extremely important from an economic as well as safety point of view.

The turbine blades may be twisted or staggered with respect to the axis of rotation, and the internal passages may be serpentine and connected by bends. In modern gas turbine blades, internal passages also have rib tabulators and pin fins for heat transfer enhancement. So, the heat transfer predictions in these geometrically complex passages are really difficult, without even considering the effects of rotation. Rotation affects the heat transfer mechanism significantly. It can impede the heat transfer in some surfaces and can enhance the heat transfer in some others. Use of stationary blade correlations for the design purpose can cause large deviation of the actual blade life from that predicted, or an excessive coolant mass flow rate leading to a decreased thermal efficiency. So, in order to understand the complete effect of rotation on the physics of fluid flow and heat transfer in turbine blade cooling internal passages analyses may be performed on simple geometries resembling the rotating turbine blade cooling passages. The assumption of a simple geometry helps focusing solely on the effects of rotation.

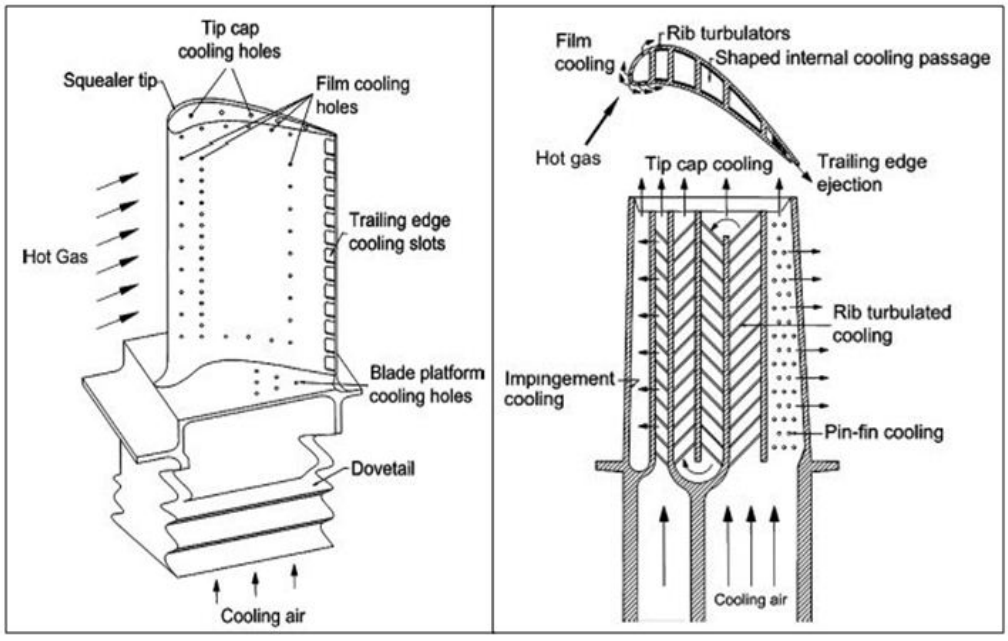

Figure 1: Schematic of a modern gas turbine blade with common cooling techniques (reproduced from [3])

1.2. LITERATURE SURVEY

The effect of rotation on the fluid flow and heat transfer in rotating ducts is of interest to engineers because of its application in turbine blade cooling. Most of these experimental studies are conducted on orthogonally rotating cooling channels with external heat input. Morris and Ayhan [4] performed an experimental study on an orthogonally rotating cylindrical tube subjected to a uniform heat flux to find the influence of Coriolis acceleration and centripetal buoyancy on the heat transfer at different Reynolds numbers and different rotational speeds. Morris and Chang [5] experimentally studied the case of rotating coolant channel with constant heat flux. They performed their experiments on a channel of constant circular cross-section to understand the complex interaction of buoyancy force and Coriolis force. They found no evidence of the traditional fully developed region. Although, they only analyzed the case of radially outward flowing coolant. Guidez [6] reported that Coriolis induced secondary flow enhances the mean heat transfer for the radially outward flow case. The local heat transfer coefficient is considerably higher near the trailing edge and slightly lower near the leading edge as compared to fully-developed non-rotating turbulent flow case, this effect weakening at high Reynolds numbers. Wagner et al [7] conducted an experimental study on smooth rectangular rotating channels with constant wall temperature for varying Reynolds number, Rossby number (inverse of the Rotation number), coolant density ratio and radius ratio for radially outward flow. The lack of heat transfer correlations was attributed to the complex interaction of stabilization, buoyancy and Coriolis effects. In the second part of his study Wagner et al [8] conducted experiments on serpentine passage to consider the effect of both radially inward flow and radially outward flowing case. The increase in mean heat transfer was found to be less for the radially inward flow as case compared to the radially outward flow case. Kuo and Hwang [9] conducted experiment on uniformly heated rotating square duct for both the cases of radially outward and radially inward flowing coolant. They also tried to explain many of the contradicting findings found on earlier works. They tried to form a general correlation for Nusselt number ratio taking into effect the direction of flow, rotation and rotational buoyancy, although no value of the constants in the correlation has been suggested. Bons and Kerrebrock [10] used particle image velocimetry (PIV) to investigate the internal flow in a single pass square duct with rotation number values up to 0.2. They reported an accumulation of hot and low momentum

coolant near the leading wall which effectively deters heat removal from that region. They also pointed out the significance of considering Coriolis force and buoyancy simultaneously for accurate heat transfer predictions. Apart from these studies, the effect of rotation on fluid flow and heat transfer for rotating coolant channel has been studied by Elfert [11], Soong [12] etc.

Heat transfer in rotating internal passages of turbine blades also depends on the geometry of the channels. Experiments have been conducted on triangular, square and rectangular channels with different aspect ratios to understand the effect of channel geometry on heat transfer and fluid flow of orthogonally rotating coolant channels by Huh et al [13], Liu et al [14] and Agarwal et al [15]. In more recent times computational fluid dynamics has been used by researchers to study the complex flow field and heat transfer in the internal cooling passages of rotor blades. A new turbulence model which includes the Coriolis and buoyancy terms has been used by Dutta et al [16] to study heat transfer characteristics in leading and trailing sides of a rectangular duct. They considered test cases at different Reynolds numbers, Grashof numbers and Rotation numbers for radially outward flowing coolant. Yan and Soong [17] numerically studied rotational effects and found that the secondary flow due to the Coriolis force raises the peripherally averaged friction factor and heat transfer. Iacovides and Launder [18] extensively reviewed the existing capability of predicting fluid flow and heat transfer characteristics using computational fluid dynamics for flow inside internal passages of turbine blades where the flow is three dimensional. Conventional gas turbine blade analysis like the one done by Cohen et al [19] considers infinite thermal conductivity and the neglects the effect of rotation. However, with the present technology of thermal barrier coatings, the resistance offered by each layer of the material needs to be taken into account.

1.3. OBJECTIVE AND SCOPE OF CURRENT STUDY

The objective of the present study is to understand the effect of rotation on the temperature of cooling air in turbine blade cooling passages, which establishes a new method of performance optimization. A simple geometry of circular cross-section (cylindrical channel) with smooth walls has been considered in order to properly understand the coupled effect of heat transfer and rotation without the additional influence of rib turbulators and pin

arrays. First, the case of only rotation without external heat transfer, i.e. from hot gases to the blade, has been analytically modeled and then verified with the results of CFD simulation. Next, the case of only heat transfer without rotation (static blade case) has been studied analytically considering finite thermal conductivity of the blade material and a corresponding conjugate heat transfer CFD analysis is used to validate the results. Finally, the coupled effects of rotation and external heat transfer have been considered both analytically and numerically. Orthogonally rotating channels, i.e. axis of rotation is perpendicular to the axis of the coolant channel, have been considered for both the cases of radially outward and inward flowing coolant. The effect of rotation induced Coriolis force and centrifugal force on the coolant temperature is also discussed. Better prediction of blade coolant relative total temperature leads to better prediction of blade temperature, hence improving blade life prediction. Effect of rotation on non-dimensional coolant mass flow rate for the radially outward and the radially inward flow case in comparison with the non-rotating (static blade) blade case is also discussed. Finally, effect of rotation number on coolant relative total temperature is investigated for both the radially outward and the radially inward flowing coolant case.

CHAPTER 2
THEORY

2.1. THEORETICAL FORMULATION

In case of internally cooled gas turbine blades, heat transfer occurs in the form: first convective heat transfer from combustion gases to the blade, then conduction through the blade material and finally convective heat transfer from the blade to the cooling air. Internal cooling passages in turbine blades rotate orthogonally with respect to the axis of rotation i.e. axis of the coolant passage is perpendicular to the axis of rotation. The flow field in rotating internal coolant passages is governed by the momentum equation but the inertia term needs to be modified to account for rotation. Although the flow is turbulent in most coolant passages, the laminar case needs to be considered first to understand the effect of rotation on the flow field. For a coolant passage with constant circular cross-section, the modified momentum equation can be written as [5],

$$\rho \frac{Dv}{Dt} + 2\rho (\omega \times v) = -\nabla p - \rho [\omega \times (\omega \times r)] + \mu \nabla^2 v \,. \tag{1}$$

The second term on the left hand side and the second term on the right hand side account for the Coriolis force and the centrifugal force respectively that come into play due to rotation. Viscosity and density of the fluid is assumed to be invariant.

2.2. CONVENTIONAL INTERNAL COOLING ANALYSIS WITHOUT THE EFFECT OF ROTATION

The case of external heat transfer is considered for a static coolant channel (that is, in the absence of rotation effects) and the modeling is extended to include the effect of finite thermal conductivity of the blade material and that of the thermal barrier coating. Considering heat transfer occurring in three steps: from the combustion gases to the blade surface by convection, then conduction of heat through the blade material and finally

convective heat transfer from the blade inner surface to the coolant, a two dimensional model of the blade element is developed (Figure 2).

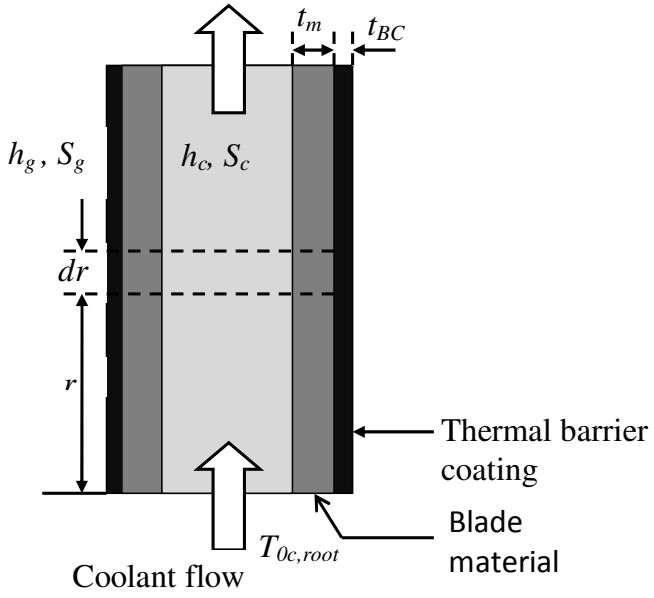

Figure 2: Schematic of internally cooled gas turbine blade

Considering an elemental strip of length *dr* and neglecting axial conduction, as blade materials usually have low thermal conductivities, we can write a heat balance equation for the element as,

$$h_g\, S_g\, (T_g - T_b) = h_c\, S_c\, (T_b - T_c)\,. \tag{2}$$

Now considering the increase in temperature of the coolant due to convective heat transfer from the inner surface of the blade to the coolant,

$$m_c\, c_{pc}\, \frac{dT_c}{dr} = h_c\, S_c\, (T_b - T_c)\,. \tag{3}$$

By eliminating T_b from equation (2) and (3) and solving for T_c we get [19],

$$T_c = T_g - (T_g - T_{c,root})\, e^{-\beta r} \tag{4}$$

where $\beta = \dfrac{h_g\, S_g\, h_c\, S_C}{m_c\, c_{pc}\, (h_g\, S_g + h_c\, S_c)}$.

The above formulation can also be derived from the fundamental steady flow energy equation by neglecting changes in kinetic and potential energies. Equation (4) is the same as given in Cohen et al [19], but one important assumption in this analysis is that of infinite thermal conductivity. With the advent of modern technologies like thermal barrier coating, finite thermal conductivity of the blade material and thermal barrier coating needs to be incorporated in the calculation. So in the above formulation h_g is replaced by U_g the overall heat transfer coefficient, where

$$U_g = \frac{1}{\left(\dfrac{1}{h_g} + \dfrac{t_{BC}}{k_{BC}} + \dfrac{t_m}{k_m} \right)}. \tag{5}$$

The final expression for coolant temperature can be written as,

$$T_c = T_g - (T_g - T_{c,root})\, e^{-\beta r} \tag{6}$$

where $\beta = \dfrac{U_g\, S_g\, h_c\, S_C}{m_c\, c_{pc}\, (U_g\, S_g + h_c\, S_c)}$.

2.3. EFFECT OF ROTATION WITHOUT EXTERNAL HEAT TRANSFER

First, only the effect of rotation is considered without any external heat transfer. Internal coolant flow through the rotating turbine blades can be modeled as orthogonally rotating channel flow,(the axis of the channel is perpendicular to the axis of rotation), with the channel being eccentric to the center of rotation as shown in Figure 3. The coolant flow through the channel is taken along the r-direction while the channel itself rotates about the y-axis. Taking a control volume around the cooling channel and applying the steady flow energy equation in differential form in an inertial frame of reference, we get

$$\frac{dq}{dr}=\frac{d\hbar}{dr}+\frac{d(KE)}{dr}+\frac{d(PE)}{dr}+\frac{dW}{dr}. \tag{7}$$

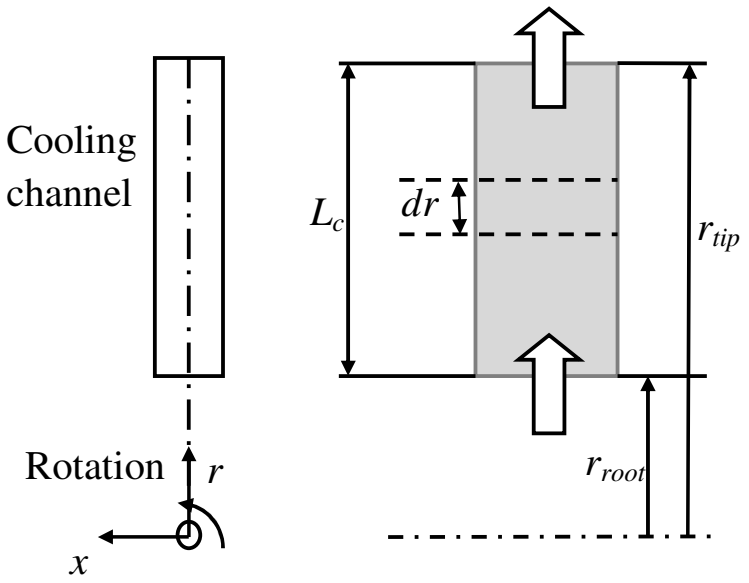

Figure 3: Schematic of the orthogonally rotating channel

Shifting to a non-inertial frame of reference which is rotating at the same speed as the rotor, the steady flow energy equation is given by

$$\frac{dq}{dr}=\frac{d\hbar}{dr}+\frac{d(KE)}{dr}+\frac{d(PE)}{dr}. \tag{8}$$

Since the rotor blades are stationary with respect to the non-inertial frame, the shaft work output is equal to zero, i.e. $dW/dr=0$. Denoting the relative velocity of the coolant in the internal cooling passage with respect to the rotating non-inertial frame by v_{rel}, the kinetic energy is expressed as

$$\frac{d(KE)}{dr}=v_{rel}\frac{dv_{rel}}{dr}. \tag{9}$$

Centrifugal potential, apart from gravitational potential, needs to be accounted for in the rotating non-inertial frame of reference, so

$$\frac{d(PE)}{dr} = g - \omega^2 r \ . \tag{10}$$

Next, by substituting equation (9) and (10) in equation (8) and neglecting changes in gravitational potential energy,

$$\frac{dq}{dr} = \frac{d\hbar}{dr} + v_{rel} \ \frac{dv_{rel}}{dr} - \omega^2 \ r \, . \tag{11}$$

As no heat transfer has been considered in this case, $dq/dr = 0$ and by introducing the term relative total enthalpy $(\hbar_{0c,rel} = \hbar + v_{rel}^2 / 2)$ in equation (11),

$$\frac{d\hbar_{0c,rel}}{dr} - \omega^2 \ r = 0 \, . \tag{12}$$

Assuming the coolant to be perfect gas and integrating both sides of equation (12),

$$T_{0c,rel} = \frac{\omega^2 r^2}{2c_p} + C \, . \tag{13}$$

$T_{0c,rel}$, the relative total temperature, can be defined as the total temperature observed by an observer attached to the non-inertial frame that is rotating at the same speed as that of the blade. C is the integration constant.

Now applying appropriate boundary conditions to equation (13) for radially outward flowing coolant, at $r = r_{root}$, $T_{0c,rel} = T_{0c,root}$ and substituting the value of the constant in equation (13),

$$T_{0c,rel} = T_{0c,root} - \frac{\omega^2 \ r_{root}^{\ 2}}{2c_p} \left[1 - \left(\frac{r}{r_{root}} \right)^2 \right] . \tag{14}$$

For radially inward flowing coolant, the boundary condition needs to be changed to: at $r = r_{tip}$, $T_{0c,rel} = T_{0c,tip}$ and substituting the value of the constant in equation (13),

$$T_{0c,rel}=T_{0c,tip}-\frac{\omega^2\, r_{tip}{}^2}{2c_p}\left[1-\left(\frac{r}{r_{tip}}\right)^2\right]. \tag{15}$$

Equation (14) and (15) are the new analytical formulation developed in this study, for radially outward and inward flowing coolant relative total temperature considering the effect of rotation (without external heat transfer) respectively. Now if zero eccentricity case is considered for a coolant channel of length L_c, then for radially outward flowing coolant in equation (14) substituting $r_{root}=0$ and $r = L_c$ it is observed that coolant relative total temperature increases by $\omega^2 L_c^2 \big/ (2c_p)$ and for radially inward flowing coolant, in equation (15) substituting $r_{tip}=L_c$ and $r=0$, it is observed that coolant temperature decreases by $\omega^2 L_c^2 \big/ (2c_p)$. As the coolant flows outward work is done on the coolant, thus raising its relative total temperature while the opposite is true for the radially inward case.

2.4. IMPROVED ANALYSIS WITH EFFECT OF ROTATION AND EXTERNAL HEAT TRANSFER

Finally the heat transfer analysis for the blade element is performed considering the effects of rotation. When rotation and external heat transfer is considered simultaneously, equation (7) reduces to

$$\frac{dq}{dr}=\frac{d\hbar_{0c,rel}}{dr}-\omega^2\, r\ . \tag{16}$$

Equation (16) differs from equation (11), in that external heat transfer is considered in the former, so $dq/dr \neq 0$, while it was set to zero in the latter. Rotation induced Coriolis force generates a secondary flow which significantly affects the fluid flow and heat transfer in orthogonally rotating coolant channels. Due to the secondary flow, heat transfer increases from some part of the blade inner surface while it decreases from some other parts of the same surface depending on the direction of fluid flow and direction of rotation. So, the coolant temperature may be expected to significantly differ from that obtained by static blade analysis. The incorporation of rotational effects improves the prediction of coolant

requirement for a prescribed blade temperature which in turn increases the thermal efficiency.

Now for the radially outward flowing coolant, equation (16) can be written as

$$\frac{d\hbar_{0c,rel}}{dr} - \omega^2 r - \frac{dq}{dr} = 0 . \tag{17}$$

Similarly for inward flowing coolant, choosing another rotating non-inertial frame of reference such that $b = r_{root} + L - r$ eqn. (17) is transformed to

$$\frac{d\hbar_{0c,rel}}{db} + \omega^2 \, [r_{root} + (L - b)] - \frac{dq}{db} = 0 . \tag{18}$$

Heat transfer to the coolant per unit mass flow rate of it is given by *dq/dr*. Compressibility of the coolant fluid needs to be considered to take into account the change in temperature due to the centrifugal force. For compressible flows, adiabatic wall temperature needs to be considered in the heat transfer calculations. For subsonic flows, adiabatic wall temperature is almost equal to total temperature [20],[21]. So in the heat transfer calculations the relative total temperature is to be considered. So,

$$\frac{dq}{dr} = \frac{U_g \, S_g \, h_c \, S_C (T_g - T_{0c,rel})}{m_c \, (U_g \, S_g + h_c \, S_c)} . \tag{19}$$

Introducing the concept of relative total temperature (assuming the coolant air to behave as a perfect gas) in equations (17) and (18) we get,

for the radially outward flowing coolant,

$$\frac{dT_{0c,rel}}{dr} - \frac{\omega^2 r}{c_{pc}} - \frac{U_g \, S_g \, h_c \, S_C (T_g - T_{0c,rel})}{m_c \, (U_g \, S_g + h_c \, S_c) c_{pc}} = 0 \tag{20}$$

and for the radially inward flowing coolant,

$$\frac{dT_{0c,rel}}{db} + \frac{\omega^2 \, [r_{root} + (L-b)]}{c_{pc}} - \frac{U_g \, S_g \, h_c \, S_C (T_g - T_{0c,rel})}{m_c \, (U_g \, S_g + h_c \, S_c) c_{pc}} = 0 . \tag{21}$$

Solution of these equations gives the variation of the coolant relative total temperature along the blade span. For the radially outward flowing case the boundary condition at the inlet $(r = r_{root})$ is specified as $T_{0c,rel} = T_{0c,root}$. Now solving equation (20) with the inlet boundary condition, we get,

$$T_{0c,rel}(r) = T_g + G(r) + [T_{0c,root} - T_g - G(r_{root})]e^{-\beta(r - r_{root})} \tag{22}$$

where, $\beta = \dfrac{U_g S_g h_c S_C}{m_c c_{pc} (U_g S_g + h_c S_c)}$ and $G(r) = \dfrac{\omega^2}{c_{pc}} \left[\dfrac{r}{\beta} - \dfrac{1}{\beta^2} \right]$.

Similarly for radially inward flowing coolant, the boundary condition at inlet (b=0) is given as $T_{0c,rel} = T_{0c,tip}$. Similar to the previous case (for radially outward flow), the following expression for the coolant relative total temperature is obtained by solving equation (21):

$$T_{0c,rel}(b) = T_g - G(b) + [T_{0c,tip} - T_g + G(0)]e^{-\beta b} \tag{23}$$

where, $G(b) = \dfrac{\omega^2}{c_{pc}} \left[\dfrac{\{r_{root} + (L - b)\}}{\beta} - \dfrac{1}{\beta^2} \right]$.

Equation (22) and (23) are the new analytical formulation developed in this study, for radially outward and inward flowing coolant relative total temperature considering the effect of blade rotation respectively. Equations (22) and (23) predict the coolant relative total temperature along the blade span for radially outward flowing coolant and radially inward flowing coolant respectively. These equations take rotational effect into consideration leading to better prediction of the coolant relative total temperature compared to a static blade analysis. These two equations point out the difference in the heat transfer mechanisms in action between the radially outward and radially inward flowing coolant cases, due to the effects of rotation. While the rotation induced centrifugal force causes an increase in the relative total temperature in the radially outward flowing coolant case, it causes a decrease in the relative total temperature for the case of radially inward flowing coolant. Apart from the centrifugal force, rotation induced Coriolis force also significantly alters the flow field. The secondary flow, induced by the Coriolis force, causes heat transfer enhancement in some

surfaces and reduce heat transfer from some surfaces. So, due to a complex interaction of these forces, the heat transfer mechanism in a rotating internal cooling channel of turbine blades becomes very difficult to predict.

Coolant outlet relative total temperature is required for calculating the cooling efficiency which is an indicator of the cooling technology in use. For a particular cooling effectiveness, the non-dimensional coolant mass flow rate required is calculated at a particular value of cooling efficiency. So, an accurate prediction of the coolant relative total temperature leads to a better prediction of coolant requirement. Over prediction of coolant flow rate causes loss in cycle efficiency, as the coolant air is extracted from the high pressure compressor. This air, extracted from the compressor, does not participate in combustion and consequently does not produce any work, thus incurring a loss in cycle efficiency. Under prediction of the coolant mass flow rate can cause higher blade metal temperature, leading to a decrease in blade life. This explains why an accurate prediction of coolant mass flow rate is of utmost importance. So, equation (22) and (23), which gives the coolant relative total temperature considering the effect of rotation, gives a better prediction of the coolant mass flow rate as compared to the static blade analysis. This leads to a better prediction of cycle efficiency and blade life.

CHAPTER 3

COMPUTATIONAL FLUID DYNAMIC APPROACH

The case of orthogonally rotating coolant duct is also computed using computational fluid dynamics (CFD) to demonstrate that the results of the theoretical analysis are in excellent agreement with the CFD predictions.

3.1. GEOMETRIC DETAILS

Mainly, two dimensionless parameters are taken into account to reproduce engine similar conditions: (i) Reynolds number (Re) and (ii) Rotation number (Ro). The Reynolds number (Re_{Dh}) based on channel hydraulic diameter D_h is defined as,

$$Re_{Dh} = \frac{\rho v D_h}{\mu}. \tag{24}$$

It represents the ratio of inertia force to viscous force. The effect of the Coriolis force is characterized by the Rotation number (Ro) which is defined as,

$$Ro = \frac{\omega D_h}{v}. \tag{25}$$

Table 1: Model geometric details

Geometry	Circular
Surface condition	Smooth
Reynolds number, Re	25,000
Rotation number, Ro	0.25
Hydraulic diameter, D_h	6.3 mm
L/D_h	12
Blade root radial distance from engine centerline	300 mm
Non dimensional mid-span radius, e/D_h	59.62

Rotation number represents the ratio of the Coriolis force to the inertia force. In the turbine blade cooling channels of modern aircraft engines, a typical value of Rotation number is 0.25 with Reynolds number around 25,000 [7]. Different parameters chosen for this study are shown in Table 1.

Incorporation of a finite thermal conductivity of the blade material in the analysis requires a corresponding conjugate heat transfer analysis. In the geometric model, blade material thickness is considered in such a way that the equivalent thermal resistance is the same as in the case of modern turbine blades with thermal barrier coating. Typical values of thickness and thermal conductivity of the blade material and the thermal barrier coating [22] are shown in the Table 2.

Table 2: Blade material properties

Material	Thickness(mm)	Thermal conductivity (W/m-K)
Blade material	2.0	26
Thermal barrier coating	0.15	1.8
Geometric model	2.0	12.5

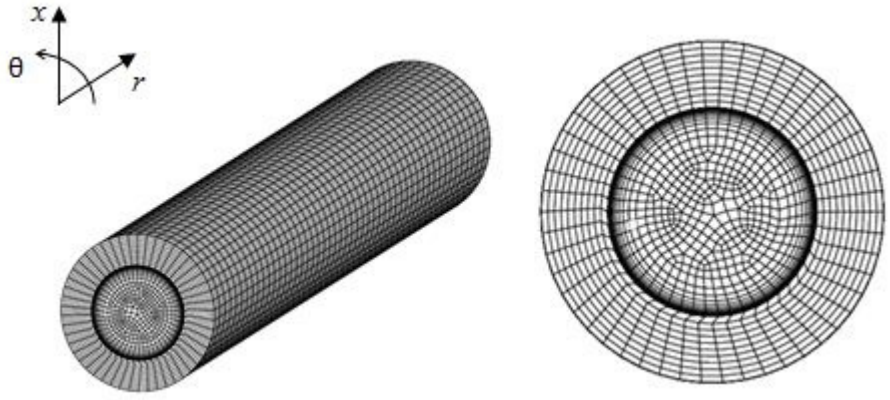

Figure 4: Geometric model and mesh used for the CFD simulation

The geometry of the model and the computational grid are generated by using the commercially available software, GAMBIT 2.4.6. 50 grid points are taken along the

periphery (in θ direction) of the coolant channel for both solid and fluid regions. In the fluid region, near-wall meshing is done using boundary layer meshing scheme with the first row distance of 1e-6 m and a successive ratio of 1.35 for 20 rows covering 1.15e-3 m radially from the wall. In the solid region uniform boundary layer type grid is used with grid spacing of 0.2e-3 m radially. Face meshing was done using Quad-Pave meshing scheme. Volume meshing is done using Cooper scheme with hexahedral elements with 50 grid points along the axial direction (in *r* direction). Figure 4 shows the mesh used for CFD simulations.

3.2. NUMERICAL METHOD

Computational fluid dynamics simulations were performed using the commercial CFD software package ANSYS FLUENT 14.0. FLUENT uses a finite volume method (FVM) for solving continuity, momentum and energy conservation equations by discretizing the spatial domain into a mesh of discrete nodes. Three dimensional, double precision, pressure based steady solver along with a relative velocity formulation is used for all the cases presented here. Standard version of the k-ε model with enhanced wall treatment is used to model the effects of turbulence, as it tackles most of the flow considerations reasonably well in case of internal cooling [18]. Momentum, energy, turbulence kinetic energy and turbulence dissipation rate equations are discretized using a second order upwind scheme and the body force weighted discretization is used for pressure. The computational grid is refined near the walls using boundary layer meshing scheme in GAMBIT to ensure proper y^+ values ($y^+<1$) near the wall, where $y^+ = yu^*/\upsilon$. Here, υ is the kinematic viscosity, u^* is the friction velocity given by $u^* = \sqrt{\tau_w/\rho}$, where τ_w is wall shear stress and ρ is the density. The SIMPLE algorithm is used for pressure-velocity coupling in the pressure correction equation. Iterations are performed till residuals for continuity, velocity, energy, turbulence kinetic energy and turbulence dissipation rate are reduced below 1e-6.

In the first case, the case of static blade analysis with finite thermal conductivity of the blade material is simulated considering conjugate heat transfer. Mass flow inlet and pressure outlet with zero gauge pressure boundary conditions are specified at the inlet and outlet. Operating pressure is specified at 10 atm. to achieve Reynolds number of 25,000 and

Rotation number of 0.25 at the inlet. In this case density is assumed to be constant, as Dittus-Boelter correlation is used in the analytical formulation and this correlation is valid for constant density fluid. In this case, zero RPM is specified to simulate the non-rotating blade. The outer boundary is specified as wall with no slip condition and a heat transfer coefficient of 7000 W/m^2-K at an ambient temperature of 1500K. Mean heat transfer coefficient of about 7000 W/m^2-K is a typical value for the gas side in modern gas turbine engines. Inlet and outlet are specified same as it was in the previous case. Near wall grid is generated such that $y^+<1$, which is adequate for conjugate heat transfer calculations [23].

Next, the effect of rotation is considered alone without any external heat transfer. Mass flow inlet and pressure outlet with zero gauge pressure boundary conditions are specified at the inlet and outlet for both the cases of radially outward flowing and radially inward flowing coolant. Wall boundary is specified as adiabatic as external heat transfer is considered zero. Operating pressure is specified at 10 atm. to achieve Reynolds number of 25,000 and Rotation number of 0.25 at the inlet. Rotating reference frame specification is used to impart rotational motion to the channel and all the effects of centrifugal force are included. A rotational speed of 10000 RPM is specified about the y-axis, which is orthogonal to the axis of the channel (z-axis). This speed is chosen such that it is similar to the rotational speed of modern gas turbines.

Finally, the case of rotation with external heat transfer is considered. So, in this case, a rotational speed of 10000 RPM is specified about the y-axis, which is orthogonal to the axis of the channel (*r*-axis), using a rotating reference frame in FLUENT. Also, the outer boundary is specified as wall with no slip condition and heat transfer coefficient of 7000 W/m^2-K at an ambient temperature of 1500K. The inlet and outlet boundary conditions remain the same as it was in previous cases for both radially outward and radially inward flowing coolant.

CHAPTER 4
RESULTS AND DISCUSSION

4.1. GRID INDEPENDENCE TEST

First, a grid independence study has been carried out for the case of rotation only (without any external heat transfer), where only fluid region is considered. For the study three meshes with 14751, 62150 and 155925 cells have been used. For the three meshes number of grid points in θ-direction and in r-direction has been increased 1.5 times from the previous case. For the coarse mesh distance of the first grid point is taken as 2e-5 m with maximum y^+ of 4.03, but for standard mesh first grid spacing of 1e-6m is taken resulting in maximum y^+ of 0.198. For all the meshes grids are generated using boundary layer meshing scheme in GAMBIT, so that near wall y^+ values are less than 5 and hence enhanced wall treatment can be used. Based on this study a mesh with 62150 cells has been used for the results presented in the present study. In Table 3 details of this grid independence test is presented.

Grid independence test 1: Effect of rotation without external heat transfer

Grid refinement	Coarse	Standard	Fine
Number of grid points in θ-direction	34	50	76
Number of grid points in r-direction	33	50	75
Distance of the first grid point from the wall	2e-5 m	1e-6 m	0.75e-6 m
Boundary layer mesh successive ratio	1.4	1.35	1.3
Number of rows in boundary layer mesh	10	20	20
Total number of grids	14751	62150	155925
Pressure drop (Pa)	155199	155166	155161

Next, a grid independence study has been carried out for the conjugate heat transfer case considering a non-rotating blade. Since conjugate heat transfer is considered here, both the fluid and the solid region need to be modeled. For the purpose of establishing grid independent solutions three meshes with 25938, 86400 and 209400 cells have been used. For the three meshes number of grid points in θ-direction and in r-direction has been increased 1.5 times from the previous case. For the coarse mesh distance of the first grid point is taken as 2e-5 m with maximum y^+ of 3.69, but for standard mesh first grid spacing of 1e-6m is taken resulting in maximum y^+ of 0.207. For all the meshes grids are generated using boundary layer meshing scheme in GAMBIT, so that near wall y^+ values are less than 5 and hence enhanced wall treatment can be used. Based on this study mesh with 86400 cells has been used for the results presented in this paper. In Table 4 details of this grid independence test is presented.

Grid independence test 2: Conventional internal cooling analysis with finite thermal conductivity of blade material without the effect of rotation (conjugate heat transfer case)

Grid refinement	Coarse	Standard	Fine
Number of grid points in θ-direction	34	50	76
Number of grid points in r-direction	33	50	75
Distance of the first grid point from the wall (fluid region)	2e-5 m	1e-6 m	0.75e-6 m
Boundary layer mesh successive ratio (fluid region)	1.4	1.35	1.3
Number of rows in boundary layer mesh (fluid region)	10	20	20
Total number of grids	25938	86400	209400
Pressure drop (Pa)	582.931	576.807	576.49

4.2. CONVENTIONAL INTERNAL COOLING ANALYSIS WITHOUT THE EFFECT OF ROTATION

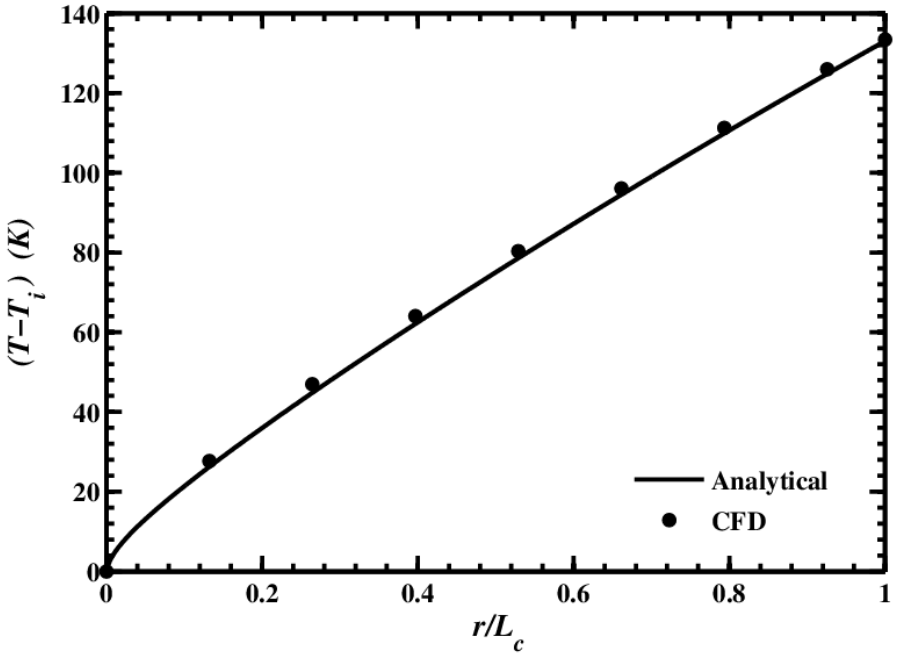

Figure 5: Comparison of increase in temperature obtained from analytical formulations and CFD for the non-rotating case (Re=25,000; Ro=0)

First, the results obtained by using the analytical expressions arising from a static blade analysis considering finite thermal conductivity of the blade material (equation (6)) is compared with the results of conjugate heat transfer analysis by CFD simulations. Figure 5 shows that the CFD predictions are in agreement with the analytical results. In equation (6), all the values are specified except for the coolant side heat transfer coefficient. The Dittus-Boelter correlation [24] for Nusselt number in fully developed turbulent smooth pipe flow has been used to find the coolant side heat transfer coefficient. Dittus-Boelter correlation is given as,

$$Nu_{nr}=0.023\mathrm{Re}_{Dh}^{0.8}\,\mathrm{Pr}^{n}. \tag{26}$$

Where, n=0.4 for heating of the fluid and n=0.3 for cooling of the fluid. As the L/D_h ratio for the current geometry is low and the flow is not fully developed, the Nusselt number correlation [25] is modified to take into account the entrance effect.

$$Nu_{nr}=0.023\left[1+\frac{C}{(x/D_h)^m}\right]\mathrm{Re}_{Dh}^{0.8}\,\mathrm{Pr}^n \tag{27}$$

where, $C=1$, $m=2/3$ and x is the distance from the inlet. All the properties are evaluated at the bulk mean temperature, where bulk mean temperature is defined as the arithmetic mean of the coolant temperature at inlet and outlet. Density of air is calculated using the ideal gas law and viscosity at the bulk mean temperature is evaluated using Sutherland's Law.

The difference between analytical results and CFD predictions may be attributed to the assumption of fully developed flow in the Dittus-Boelter correlation. Also the fact CFD uses discretized transport equations and turbulence modeling, is responsible for introducing approximations which lead to some deviation from the real physical phenomenon.

4.3. EFFECT OF ROTATION WITHOUT EXTERNAL HEAT TRANSFER

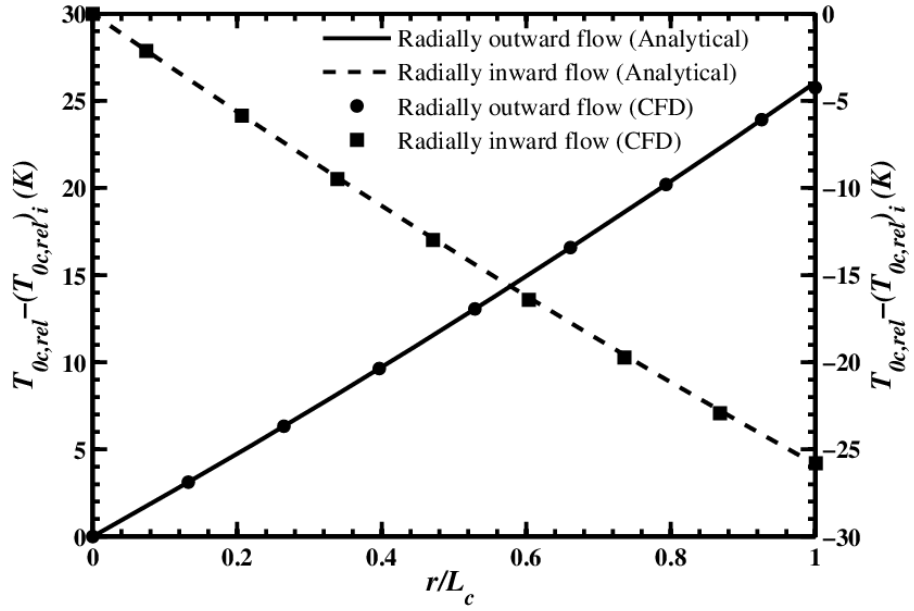

Figure 6: Comparison of change in relative total temperature obtained from analytical formulation and CFD simulation for radially outward flowing case and radially inward flowing case (Re=25,000; Ro=0.25)

Next, results obtained from CFD simulation are compared with analytical expressions obtained in equations (14) and (15) for radially outward and radially inward flowing cases

respectively. For the case when rotation is considered separately Figure 6 shows that the CFD predictions are in good agreement with the analytical formulations, i.e. equations (14) and (15) respectively. For both the plots 0 denotes the inlet and 1 denotes the outlet although the physical locations of inlet and outlet are different for both the cases. For the radially outward flow case, work is done on the fluid due to the centrifugal force, thus raising its relative total temperature; however, in the case of radially inward flowing coolant, work is done by the fluid against the centrifugal force, thus resulting in a decrease in its relative total temperature. It must be kept in mind that CFD uses discretized transport equations and turbulence modeling which introduce approximations to the actual physical phenomenon.

4.4. EFFECT OF ROTATION WITH EXTERNAL HEAT TRANSFER

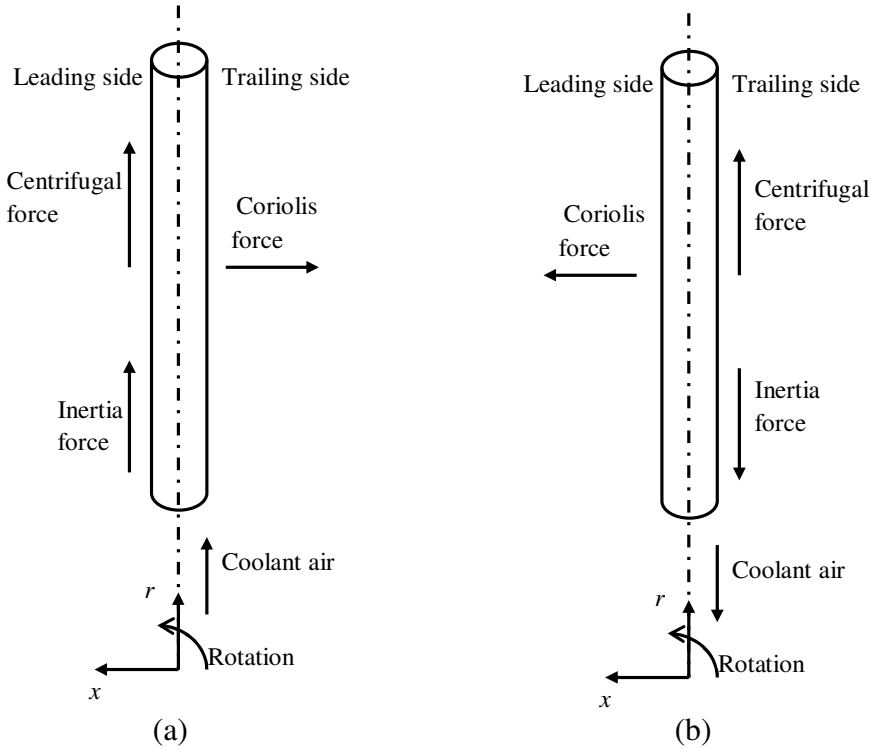

Figure 7: Schematic of rotating coolant channel configuration and direction of different forces for (a) radially outward and (b) radially inward flowing coolant

Finally, the case of rotation with external heat transfer is considered. Before proceeding further the physics of the fluid flow and heat transfer needs to be understood properly. For the case of heat transfer in orthogonally rotating coolant channels, the cooling fluid is subjected to an inertia force, a rotation induced centrifugal force and a Coriolis force. The

inertia force is along the mainstream flow direction, the centrifugal force acts in the radially outward sense for both the cases of radially outward flowing coolant and radially inward flowing coolant and the Coriolis force is perpendicular to the direction of mainstream flow with a sense depending on the direction of rotation and mainstream flow direction. Figure 7 shows the direction and sense of these forces for both the cases of radially outward flowing coolant and radially inward flowing coolant.

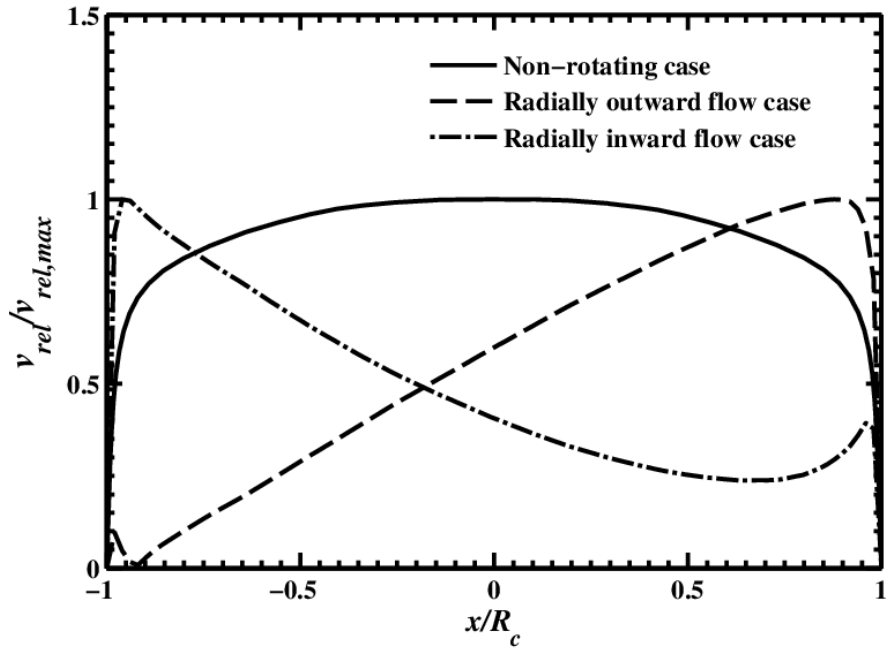

Figure 8: Comparison of relative velocity profile for non-rotating case, rotating radially outward flow and radially inward flow: prediction of present CFD computation

In Figure 8, the normalized relative velocity at the outlet is plotted against the non-dimensional distance for three cases have been compared: non-rotating channel, rotating channel with radially outward flow and rotating channel with radially inward flowing coolant. In the figure, left side of the x-axis is the leading side while the trailing side is on the right. R_c is the cooling channel radius. It is quite evident from the figure that the velocity profile for the case of radially outward flowing coolant is skewed towards the trailing side. For the radially inward flowing case, the direction of Coriolis force is such that core flow is pushed towards the leading side. So the velocity profile should be skewed towards the leading side of the channel. However, the velocity profile for both the cases are not of similar nature as can be seen from Figure 8**.** For the radially inward flowing coolant, while the

centrifugal force still acts radially outwards, the inertia force acts radially inward. So due to inertia the heavier mass of fluid near the leading side is pushed towards the root of the blade, while the centrifugal force tries to decelerate the flow near the leading side. As a result, for the radially inward flowing case, the relative velocity profile is not as skewed towards the direction of Coriolis force as it was in case of the radially outward flowing coolant. This phenomenon, although described briefly by Han et al [26], has not been investigated previously in any detail.

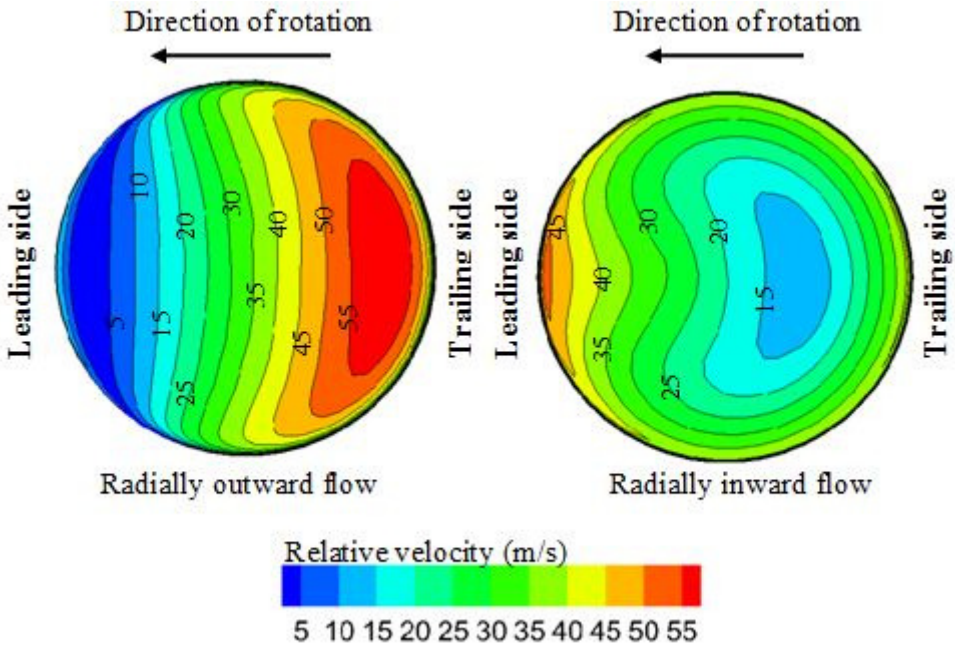

Figure 9: Mid-span relative velocity magnitude contour for (a) radially outward and (b) radially inward flow case respectively: prediction of present CFD computation (Re=25,000; Ro=0.25)

In Figure 9, the relative velocity contours at the mid-span of the coolant channel for both radially outward and inward flowing cases have been compared. For the radially outward flowing case, the Coriolis force pushes the core flow towards the trailing side, while in case of radially inward flowing coolant the Coriolis force pushes the core fluid towards the leading side. A closer observation of the relative velocity contours for both the cases reveals that the velocity contour is not as skewed for the radially inward flow case as it is in case of radially outward flowing coolant. This is because the direction of the forces depends on the direction of the coolant flow which makes the flow field for the radially outward flowing

case different from that of the radially inward flowing case. Due to such a complex interaction of these forces, the fluid flow and heat transfer characteristics become quite complex for orthogonally rotating channel with the direction of flow emerging as a major influencing factor.

A proper understanding of the effects of rotation induced centrifugal force and Coriolis force on the fluid flow helps to understand the effect of these forces on heat transfer. For radially outward flow Coriolis force pushes the core flow towards the trailing side. So, the velocity near the trailing side is increased and at the same time the flow velocity is very low near the leading side. Due to this, the heat transfer coefficient at the leading side is less than that for the non-rotating channel case. The Nusselt number ratio is defined as the ratio of the Nusselt number for the rotating case to the Nusselt number for fully developed turbulent pipe flow(non-rotating case) as given by the Dittus-Boelter correlation.

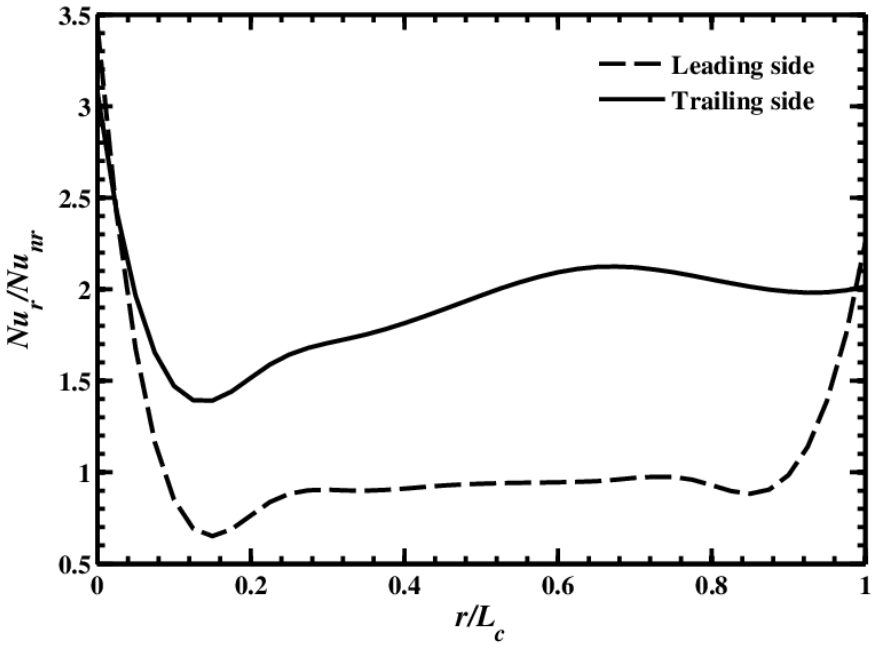

Figure 10: Nusselt number ratio at the leading and trailing side for radially outward flow: prediction of present CFD computation (Re=25,000; Ro=0.25)

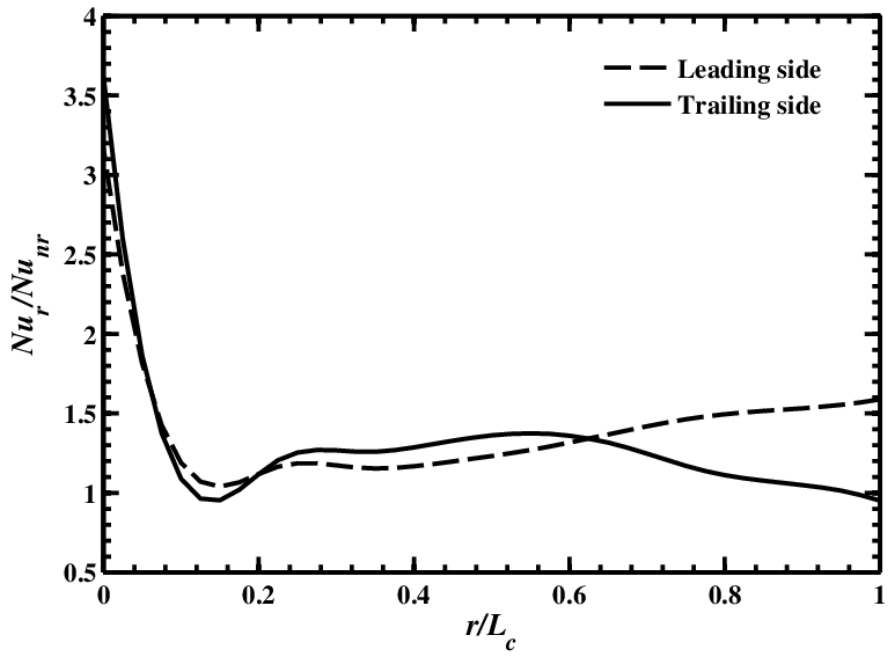

Figure 11: Nusselt number ratio at the leading side and trailing side for radially inward flow: prediction of present CFD computation (Re=25,000; Ro=0.25)

In Figure 10, the Nusselt number ratio for the radially outward flowing case at the leading side has been compared to that at the trailing side. For the radially inward flow case, the Coriolis force pushes the core flow towards the leading side, thus leading to an increased velocity there. This phenomenon results in a higher Nusselt number ratio near the leading side compared to that near the trailing side. Figure 11 shows a comparison of the Nusselt number ratio at the leading side and the trailing side for radially inward flow case. For both Figures 10 and 11, zero denotes the inlet and one denotes the outlet. For the case of radially inward coolant flow, the trailing side heat transfer coefficient near the outlet is found to be less than that in the non-rotating case. These results are in qualitative agreement with the experimental findings of Wagner et al ([7] and [8]).

Figures 10 and 11, show the difference in heat transfer mechanism between the orthogonally rotating case and the non-rotating case. Parametric studies to predict the heat transfer mechanism in orthogonally rotating coolant channels have been performed by many researchers. They reported the Nusselt number ratio variations along the length of the channel for different values of the parameters involved. However, for coolant mass flow rate calculations, the mean heat transfer needs to be considered. To predict the efficiency of the

cooling technology, coolant temperature is of prime importance since it dictates the coolant mass flow rate required. The heat transfer coefficient varies along the length of the channel and from the leading side to the trailing side depending on the direction of main through flow and the direction of rotation. Therefore, in the analytical expressions in equations (22) and (23), the mean heat transfer coefficient needs to be considered.

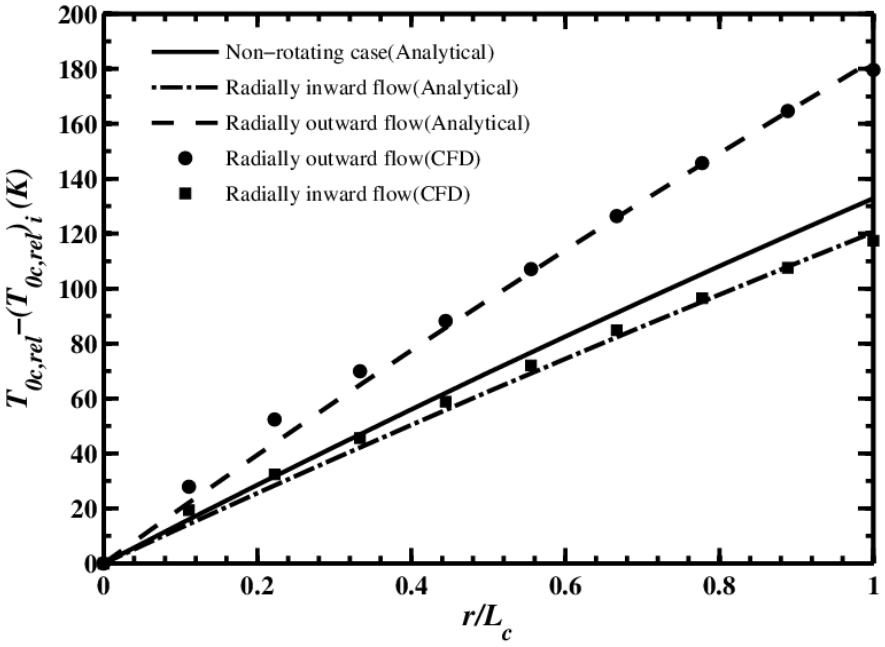

Figure 12: Comparison of change in relative total temperature obtained from analytical formulations and CFD simulation for non-rotating case, radially outward flow and radially inward flow case: prediction of present CFD computation

In Figure 12, changes in the relative total temperature obtained from theory (equations (22) and (23)) and that predicted by CFD simulations have been compared for three different cases (non-rotating channel, rotating radially outward and radially inward flows). In the analytical expressions, the values of surface average Nusselt number ratio given by CFD simulations have been used for calculating the coolant side heat transfer coefficient. For the Nusselt number ratio calculations, the bulk temperature is assumed to be varying linearly from the inlet to the outlet. Deviation of the theoretical results and the predictions of CFD simulations near the inlet may be attributed to the entrance effect. Apart from the inlet region, theoretical predictions of change in relative total temperature given by equations (22) and (23) are in agreement with CFD simulation results.

When rotation is involved, the heat transfer is influenced by centrifugal and Coriolis forces. While the Coriolis force generated secondary flow tends to increase the heat transfer for both cases of radially outward flow and radially inward flow, effect of the centrifugal force depends on the direction of the main through flow. For the radially outward flow case, the centrifugal force tends to increase the relative total temperature while for the radially inward flow case it decreases the relative total temperature from inlet to outlet. Hence, for radially outward flow in the rise in the relative total temperature is aided by both the forces. On the other hand, for the radially inward flow case the Coriolis force tends to increase the relative total temperature while the centrifugal force tends to decrease it. As a result increase in the relative total temperature for the latter case is not significantly different from that in the non-rotating case. The relative strength of these two forces and the inertia force influence the heat transfer characteristics and determines how rotation affects the coolant relative total temperature.

Before going further with the analysis few of the frequently used terms in cooling flow calculations described below [27],

Cooling efficiency (η) is defined as,

$$\eta = \frac{\left(T_{0c,rel}\right)_o - \left(T_{0c,rel}\right)_i}{T_{b,m} - \left(T_{0c,rel}\right)_i} \tag{28}$$

Cooling effectiveness (ε) is defined as,

$$\varepsilon = \frac{T_g - T_{b,m}}{T_g - \left(T_{0c,rel}\right)_i} \tag{29}$$

Non dimensional mass flow rate (m^*) is defined as,

$$m^* = \frac{\varepsilon}{\eta(1-\varepsilon)} \tag{30}$$

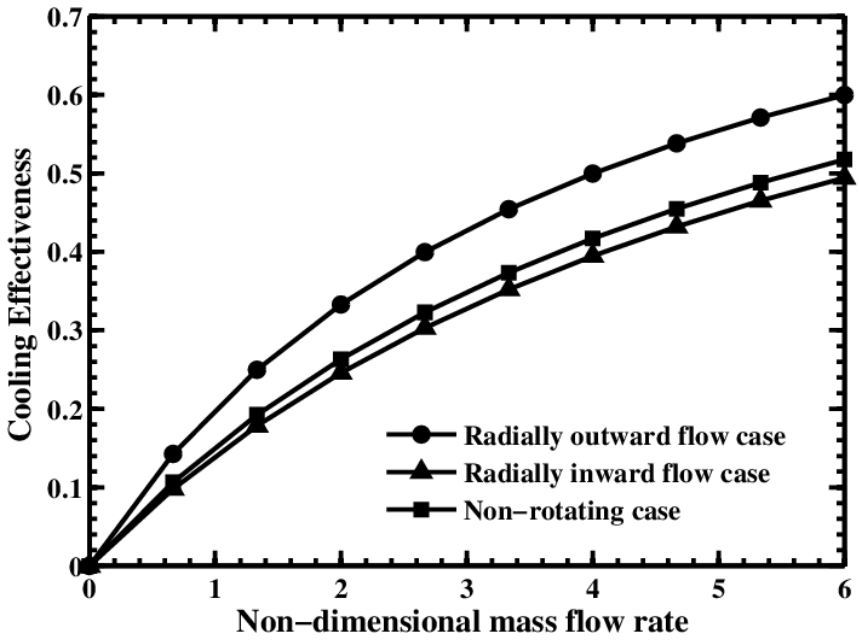

Figure 13: Comparison of variation of convective effectiveness as a function of non-dimensional coolant flow, for non-rotating case, radially outward flow and radially inward flow case: prediction of present CFD computation

In Figure 13, the cooling effectiveness (ε) is plotted against the non-dimensional mass flow rate for the three cases considered in the present study. It can be seen that, for the same cooling effectiveness, using the non-rotating blade analysis for predicting the cooling efficiency leads to an over prediction of the coolant flow requirement in case of radially outward flowing coolant. This over prediction of coolant air requirement in turn reduces the thermal efficiency as the air, taken out from the later stages of the compressor, does not take part in combustion and hence produces no work. Also for the radially inward flowing case, the non-rotating blade analysis under predicts the coolant flow requirement for the same cooling effectiveness. This under prediction may lead to component damage and could reduce blade life. So, the theory presented here improves the predictions of the static blade analysis by incorporating the effects of rotation on the coolant relative total temperature, which leads to a better prediction of coolant flow requirement.

To understand the effect of rotation on coolant relative total temperature, a parametric study needs to be performed at different rotation speeds. For this purpose, simulations are performed at 10000, 7500, 5000 and 2500 rpm, which corresponds to rotation numbers of

0.25, 0.1875, 0.125 and 0.0625 respectively. Analytical formulation derived in equation (22) and (23) for radially outward and inward flowing coolant is found to be in reasonable agreement with the surface averaged heat transfer characteristics of the CFD computation. In the analytical formulations the coolant side heat transfer coefficient is different from that predicted by Dittus-Boelter correlation due to the effect of rotation. So, CFD computations are performed at four different rotational speeds of 10000, 7500, 5000 and 2500 rpm for both cases of radially outward and radially inward flowing coolant. Surface averaged Nusselt number ratio determined from the CFD computations then used to determine the coolant side heat transfer coefficient.

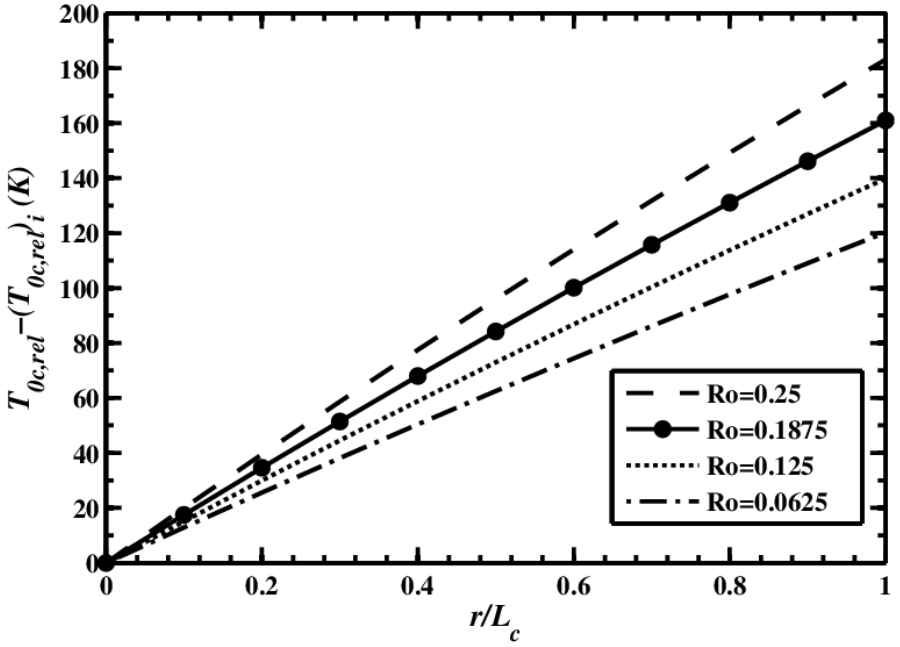

Figure 14: Change in relative total temperature for the radially outward flowing coolant case at different rotation numbers

In figure 14, change in relative total temperature for the radially outward flowing coolant case has been compared at different rotation numbers of 0.25, 0.1875, 0.125 and 0.0625. With increasing rotation number coolant relative total temperature is found to be increasing suggesting enhanced heat transfer characteristics. Increase in coolant relative total temperature for radially outward flowing coolant case, is due to two reasons. Both centrifugal force and the Coriolis force generated secondary flow increases the coolant relative total temperature.

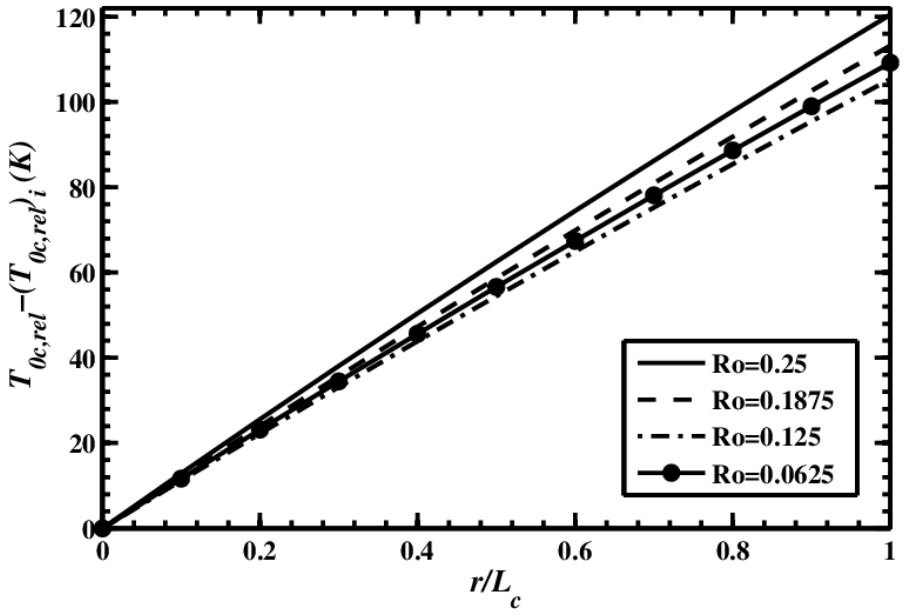

Figure 15: Change in relative total temperature for the radially inward flowing coolant case at different rotation numbers

In figure 15, change in relative total temperature for the radially inward flowing coolant case has been compared at different rotation numbers of 0.25, 0.1875, 0.125 and 0.0625. With increasing rotation number coolant relative total temperature is found to be increasing. Closer observation reveals increase in coolant relative total temperature is not that significantly varying at different rotation numbers for radially inward flowing case as it is in case of radially outward flowing coolant case. In case of radially inward flowing coolant while the Coriolis force generated secondary flow enhances the overall heat transfer characteristics, coolant relative total temperature decreases due to the effect of centrifugal force. Due to these two opposing effect of rotation number or rotational speed is not that significant for radially inward flowing coolant case.

Another interesting observation is that, coolant relative total temperature in case of Ro=0.125 is found to be less than that at Ro=0.0625. This is because at higher rotation number or rpm while the heat transfer enhancement due to coriolis generated secondary flow is more, but at the same time due to higher rpm or rotation number drop in coolant relative total temperature from inlet to outlet is also more. At Ro=0.25 drop in coolant relative total temperature is significantly more than the enhancement in heat transfer characteristics due to

coriolis force generated secondary flow. For this reason, coolant relative total temperature at Ro=0.125 is found to be less than that in case of Ro=0.0625.

CHAPTER 5
CONCLUSION

The present work attempts to understand the effect of rotation on the coolant relative total temperature in orthogonally rotating turbine internal coolant channels. The effects of rotation and external heat transfer have been studied separately and then combined to model the actual situation closely.

1. If only rotation is considered for the orthogonally rotating coolant channel then, the relative total temperature for radially outward flow case increases from inlet to outlet, while it decreases for the radially inward flow case. Figure 6 establishes the validity of the new analytical formulation for effect of rotation without external heat transfer, equation (14) and (15).

2. Conventional analysis for static internal blade cooling has been extended to include the effects of finite thermal conductivity of the blade material and corresponding CFD simulations have been performed to validate the theory. Figure 5 establishes the validity of the analytical formulation for non-rotating blade analysis without rotation, equation (6).

3. Finally, the effect of rotation with external heat transfer for orthogonally rotating coolant channel has been considered and analytical expressions have been derived which improve the static blade analysis by incorporating effects of rotation on the coolant relative total temperature. Figure 12 establishes the validity of the new analytical formulation for effect of rotation with external heat transfer, equation (22) and (23).

4. The secondary flow generated by the Coriolis force is found to increase the mean heat transfer as compared to the non-rotating case.

5. Due to the combined effects of Coriolis force, centrifugal force and inertia force, heat transfer coefficients vary along the leading and trailing sides depending on the direction of the Coriolis force for both the cases of radially outward flowing and radially inward flowing case.

6. Change in the coolant relative total temperature from inlet to outlet for the radially outward flowing case is significantly different from that of the non-rotating case, but for radially inward flowing case, this difference is not that significant due to a complex interaction of the forces involved.

7. Using the static blade analysis for predicting the coolant flow requirement leads to an over prediction of the coolant requirement for radially outward flowing case and under prediction in case of radially inward flowing case for same cooling effectiveness. Analytical formulations suggested here improve the predictions of the static blade analysis by incorporating effects of rotation and also improves coolant mass flow requirement predictions.

REFERENCES

[1] A. Guha, "Performance and optimization of gas turbines with real gas effects," *Proceedings of the Institution of Mechanical Engineers, Part A: Journal of Power and Energy*, vol. 215, no. 4, pp. 507–512, Jan. 2001.

[2] A. Guha, "Optimisation of aero gas turbine engines," *Aeronautical Journal*, vol. 105, no. 1049, pp. 345–358.

[3] J.-C. Han, "Fundamental Gas Turbine Heat Transfer," *Journal of Thermal Science and Engineering Applications*, vol. 5, no. 2, p. 021007, May 2013.

[4] W. D. Morris and T. Ayhan, "Observations on the influence of rotation on heat transfer in the coolant channels of gas turbine rotor blades," *ARCHIVE: Proceedings of the Institution of Mechanical Engineers 1847-1982 (vols 1-196)*, vol. 193, no. 1979, pp. 303–311, Mar. 1979.

[5] W. D. Morris and S. W. Chang, "An experimental study of heat transfer in a simulated turbine blade cooling passage," *International Journal of Heat and Mass Transfer*, vol. 40, no. 15, pp. 3703–3716, Oct. 1997.

[6] J. Guidez, "Study of the Convective Heat Transfer in a Rotating Coolant Channel," *Journal of Turbomachinery*, vol. 111, no. 1, p. 43, Jan. 1989.

[7] J. H. Wagner, B. V. Johnson, and T. J. Hajek, "Heat Transfer in Rotating Passages With Smooth Walls and Radial Outward Flow," *Journal of Turbomachinery*, vol. 113, no. 1, p. 42, Jan. 1991.

[8] J. H. Wagner, F. C. Kopper, and B. V Johnson, "Heat transfer in rotating serpentine passages with smooth walls," *Journal of Turbomachinery*, vol. 113, no. 3, pp. 321–330, 1991.

[9] C. R. Kuo and G. J. Hwang, "Experimental Studies and Correlations of Radially Outward and Inward Air-Flow Heat Transfer in a Rotating Square Duct," *Journal of Heat Transfer*, vol. 118, no. 1, p. 23, Feb. 1996.

[10] J. P. Bons and J. L. Kerrebrock, "1998 Heat Transfer Committee Best Paper Award: Complementary Velocity and Heat Transfer Measurements in a Rotating Cooling Passage With Smooth Walls," *Journal of Turbomachinery*, vol. 121, no. 4, p. 651, Oct. 1999.

[11] M. Elfert, "The effect of rotation and buoyancy on flow development in a rotating circular coolant channel with radially inward flow," *Experimental Thermal and Fluid Science*, vol. 9, no. 2, pp. 206–214, Aug. 1994.

[12] C. Y. Soong, “Thermal buoyancy effects in rotating non-isothermal flows,” *International Journal of Rotating Machinery*, vol. 7, no. 6, pp. 435–446, 2001.

[13] M. Huh, J. Lei, Y.-H. Liu, and J.-C. Han, “High Rotation Number Effects on Heat Transfer in a Rectangular (AR=2:1) Two-Pass Channel,” *Journal of Turbomachinery*, vol. 133, no. 2, p. 021001, 2011.

[14] Y.-H. Liu, M. Huh, J.-C. Han, and H.-K. Moon, “High Rotation Number Effect on Heat Transfer in a Triangular Channel With 45 deg, Inverted 45 deg, and 90 deg Ribs,” *Journal of Heat Transfer*, vol. 132, no. 7, p. 071702, 2010.

[15] P. Agarwal, S. Acharya, and D. E. Nikitopoulos, “Heat Transfer in 1:4 Rectangular Passages With Rotation,” *Journal of Turbomachinery*, vol. 125, no. 4, p. 726, 2003.

[16] S. Dutta, M. J. Andrews, and J.-C. Han, “Prediction of turbulent heat transfer in rotating smooth square ducts,” *International Journal of Heat and Mass Transfer*, vol. 39, no. 12, pp. 2505–2514, Aug. 1996.

[17] W. M. Yan and C. Y. Soong, “Simultaneously developing mixed convection in radially rotating rectangular ducts,” *International Journal of Heat and Mass Transfer*, vol. 38, no. 4, pp. 665–677, Mar. 1995.

[18] H. Iacovides and B. E. Launder, “Computational fluid dynamics applied to internal gas-turbine blade cooling: a review,” *International Journal of Heat and Fluid Flow*, vol. 16, no. 6, pp. 454–470, Dec. 1995.

[19] H. Cohen, G. F. C. Rogers, H. I. H. Saravanamuttoo, and H. I. H. (r. . Saravanamutto, “Gas turbine theory,” 1996.

[20] A. H. Shapiro, “The dynamics and thermodynamics of compressible fluid flow,” *New York: Ronald Press, 1953-54*, vol. 1, 1953.

[21] A. H. Shapiro, “The dynamics and thermodynamics of compressible fluid flow (vol2),” 1954.

[22] J. Doyle and N.Mudford, “Modelling and Optimisation of Film Cooling for a Turbine Aerofoil,” University of Bristol, 2005.

[23] D. Bohn, U. Kruger, and K. Kusterer, “Conjugate heat transfer: an advanced computational method for the cooling design of modern gas turbine blades and vanes,” *Developments In Heat Transfer*, vol. 8, pp. 58–108, 2001.

[24] F. W. Dittus and L. M. K. Boelter, “Heat transfer in automobile radiators of the tubular type,” *International Communications in Heat and Mass Transfer*, vol. 12, no. 1, pp. 3–22, 1985.

[25] F. P. Incropera, *Introduction to Heat Transfer*. John Wiley & Sons, 2011, p. 960.

[26] M. Huh and J.-C. Han, "Recent Studies in Turbine Blade Internal Cooling," *Heat Transfer Research*, vol. 41, no. 8, pp. 803–828, 2010.

[27] M. J. Holland and T. F. Thake, "Rotor blade cooling in high pressure turbines," *Journal of aircraft*, vol. 17, no. 6, pp. 412–418, 1980.

[28] ANSYS Fluent, "14.0 User's Manual," *ANSYS Inc., Canonsburg, PA*, 2011.

APPENDIX

(a) Solution for Radially Outward Flowing Coolant Case

Equation (20) can be written in the form:

$$\frac{dT_{0c,rel}}{dx} - \frac{\omega^2 r}{c_{pc}} - \beta(T_g - T_{0c,rel}) = 0 \tag{A1}$$

where $\beta = \dfrac{U_g S_g h_c S_c}{m_c C_{pc}(U_g S_g + h_c S_c)}$

Equation (A1) can be written in the form,

$$\frac{dy}{dr} + P(r)\,y = Q(r) \tag{A2}$$

Where $y = T_{0c,rel}$, $P = \beta$, $Q(r) = \beta Tg + \dfrac{\omega^2 r}{c_{pc}}$.

Solution of an ordinary differential equation of the above form is: $ye^{\int Pdr} = \int Qe^{\int Pdr}dr + C$

where C is a constant

$$\int Pdr = \beta r \tag{A3}$$

$$\int Qe^{\int Pdr}dr = \int\left(\beta Tg + \frac{\omega^2 r}{C_{pc}}\right)e^{\beta r}dr = e^{\beta r}\left[T_g + \frac{\omega^2}{C_{pc}}\left(\frac{r}{\beta} - \frac{1}{\beta^2}\right)\right] + C \tag{A4}$$

The solution is of the form: $ye^{\int Pdr} = \int Qe^{\int Pdr}dr + C$. Substituting the values of each term [using (A3) and (A4)], dividing by $e^{\beta r}$, and using the condition that,

at $r = r_{root}$, $T_{0c,rel} = T_{0c,root}$, we get:

$$T_{0c,rel}(r)=T_g+G(r)+[T_{0c,root}-T_g-G(r_{root})]e^{-\beta(r-r_{root})} \quad \text{(A5)}$$

where $G(r)=\frac{\omega^2}{c_{pc}}\left[\frac{r}{\beta}-\frac{1}{\beta^2}\right]$

$T_{0c,root}$ =Coolant total temperature at the blade root.

(b) Solution for Radially Inward Flowing Coolant Case

Equation (21) can be written in the form:

$$\frac{dT_{0c,rel}}{db}+\frac{\omega^2\,[r_{root}+(L-b)]}{c_{pc}}-\beta(T_g-T_{0c,rel})=0 \quad \text{(A6)}$$

where $\beta=\frac{U_g S_g h_c S_c}{m_c C_{pc}(U_g S_g+h_c S_c)}$

Eqn (A6) can be written in the form

$$\frac{dy}{db}+P(b)\,y=Q(b) \quad \text{(A7)}$$

where, $y=T_{0c,rel}$, $P=\beta$, $Q(b)=\beta T_g-\frac{\omega^2}{C_{pc}}[r_{root}+(L-b)]$.

Solution of an ordinary differential equation of the above form is: $ye^{\int Pdb}=\int Qe^{\int Pdb}db+C$

where C is a constant

$$\int Pdb=\beta b \quad \text{(A8)}$$

$$\int Qe^{\int Pdb}=e^{\beta b}\left[T_g-\frac{\omega^2}{C_{pc}}\left(\frac{[r_{root}+(L-b)]}{\beta}+\frac{1}{\beta^2}\right)\right]+C \quad \text{(A9)}$$

The solution is of the form: $ye^{\int Pdb} = \int Qe^{\int Pdb} db + C$. Substituting the values of each term [using (A8) and (A9)], dividing by $e^{\beta b}$, and using the condition that,

at $b = 0$, $T_{0c,rel} = T_{0c,tip}$, we get:

$$T_{0c,rel}(b) = T_g - G(b) + [T_{0c,tip} - T_g + G(0)]e^{-\beta b} \tag{A10}$$

where $G(b) = \frac{\omega^2}{c_{pc}} \left[\frac{\{r_{root} + (L-b)\}}{\beta} - \frac{1}{\beta^2} \right]$

$T_{0c,tip}$=Coolant total temperature at the blade tip.